Computer Simulations of Gel Filtration Chromatograms of Rapidly Self-Associating Systems

Noriaki FUNASAKI,* Sakae HADA, and Saburo NEYA
Kyoto Pharmaceutical University, Yamashina-ku, Kyoto 607
(Received August 8, 1988)

A computer simulation method for gel filtration chromatography (GFC), based on plate theory and mass action law, is developed for rapidly self-associating systems and compared with asymptotic theory. For ovalbumin, a non-associable protein, whose elution volume increases linearly with increasing concentration, the leading boundary is predicted to be broader than the trailing. Computer simulations are used to estimate the aggregation numbers and the equilibrium constants for dimerization of carbonylhemoglobin and hexamerization of α-chymotrypsin. The concentration, C_{min}, at the plateau region of the trailing boundary is shown to be close to cmc by asymptotic theory. The present computer simulation and derivative GFC patterns serve to estimate monomer concentration and micellar size of surfactants from analysis of GFC data.

Gel filtration chromatography (GFC) is routinely used for separation of materials different in size and for estimation of the molecular weights of proteins and synthetic polymers. GFC patterns for self-associating or complex forming systems are often complicated and troublesome for the above purposes. An appropriate analysis of these systems, however, may provide useful information on molecular association. The dissociation of the hemoglobin subunits is an instance for such applications.[1] Since the assumption of a sharp (no broadening) boundary simplifies the analysis of complicated patterns for chemically reacting systems, this assumption (hereafter called asymptotic theory) has been used for analyses of GFC, sedimentation velocity,[2] and electrophoretic data. These analyses have established the stoichiometry of the reactions by using mass action law.[1-4] Furthermore, these transport properties are often represented as derivative patterns. These patterns have been analyzed by the asymptotic theory.[2-4]

The GFC method has also been used to investigate the aggregation properties of surfactants,[5] such as the aggregation number,[6] monomer concentration,[7,8] micellar size,[8-10] and mixed micelle formation.[11,12] However, since the aggregation number of surfactants is usually much larger than that of proteins, GFC elution curves of the surfactants have been analyzed on the basis of phase separation model intuitively,[8] by the asymptotic theory,[7] or by plate theory.[12,13] As a result, different analyses have been done for surfactants and proteins. For micellization of surfactants, mass action model is superior to the phase separation model; e.g., it is suggested by GFC that monomer concentration of a surfactant increases with increasing surfactant concentration above the critical micelle concentration (cmc).[7,8] Therefore the above-mentioned results for surfactants[5-13] should be analyzed in terms of the mass action model by reference with those of proteins. Furthermore, derivative GFC profiles often provide more detailed information than original profiles. No derivative GFC pattern except ours has been reported for surfactants.[10]

The major advantage of the asymptotic theory is that analytical solutions of the characteristic constants of self-associating systems are obtained from the elution curve and its derivative. Therefore this theory has been applied to surfactants and proteins.[1-7] Computer simulation procedures of transport properties (including GFC) of self-associating systems have been published.[14] These procedures require a number of parameters involved in column beds and materials used. Plate theory[15] based on the phase separation model has been applied to surfactants.[12,13] This theory is superior to the asymptotic theory, since the former predicts a more realistic profile than the latter. Another advantage of the plate theory over other theories[14] is that the adjustable parameter for the column characteristics is only the number of plates.

In the present work, we developed plate theory based on mass action model, demonstrated its usefulness for simulations of GFC profiles of proteins and surfactants, and revealed the scope and limitations of the asymptotic theory.

Computational Methods

Plate Theory. A gel column is assumed to be composed of n plates as shown schematically in Fig. 1. Each plate consists of the mobile and stationary phases. The total volume of the mobile phase equals to the void volume V_0 of the column. When a solution of volume of V_f is applied from the "zero-th" plate (the top) of the column, the mobile phase of volume V_f is flown down to the nearest neighboring plate throughout the column till another solution of the same volume flows from the n-th plate (the bottom). Then we assumed a rapid establishment of the partition equilibrium of the solute between the mobile and stationary phases at each plate.[12,13,15]

When the partition equilibrium has been established after addition of a solution of volume iV_f, the total amount of the solute at the j-th plate may be written as

$$(M_{i,j}+S_{i,j})V_f=(M_{i-1,j-1}+S_{i-1,j})V_f. \quad (1)$$

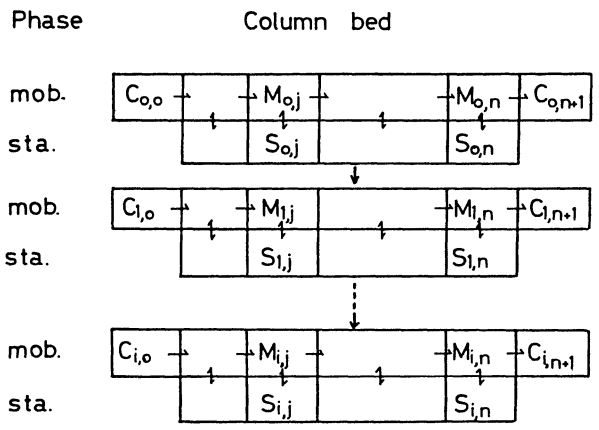

Fig. 1. Schematic elution process based on plate theory. The integers i and j indicate the numbers of transfer and plate, respectively.

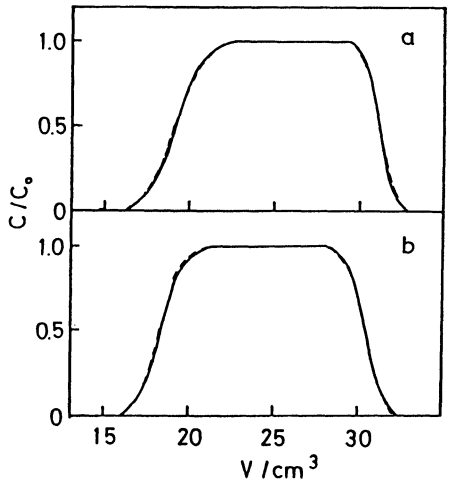

Fig. 2. Effects of concentration dependence of elution volumes upon the protein distribution for ovalbumin at (a) 12.0 g dm^{-3} and (b) 1.6 g dm^{-3}. The observed results (solid lines) are taken from Ref. 19 and the dashed lines are calculated from plate theory by using the following parameters; V_0=12.53 cm^3, n=250, and P=0.00638C_0+0.45092.

Here $M_{i,j}$ and $S_{i,j}$ are "concentrations" at the j-th plate in terms of the volume of the mobile phase (V_f). The same equilibration is made for all plates (j=1 to n). In Eq. 1, for the first plate (j=1) $M_{i-1,0}=C_{i-1,0}$ and for the n-th plate $M_{i-1,n}=C_{i,n+1}$. This procedure is repeated for different numbers of transfer (i=1 to i) starting from zero. The relation between $C_{i,n+1}$ and iV_f presents the theoretical elution curve. The partition ratio, P, of a solute between the stationary and mobile phases may be written as

$$P=S_{i,j}/M_{i,j}=(V_e-V_0)/V_0, \tag{2}$$

where V_e is the elution volume of the solute.

For analysis of GFC data two methods for charging a sample are used, viz., the small size (zonal) method and the large sample size (frontal) method.[16] The latter examples are shown in Fig. 2. When an enough volume of solution at concentration C_0 is charged, the solution of the same concentration C_0 appears on the elution curve. If a small volume of the sample is charged, the sample is diluted during elution in the column. Therefore, since the zonal method cannot be used for quantitative analysis of elution curves for self-associating systems,[9] we will consider only the frontal method. For the frontal method we may assume $C_{i,0}=C_0$ for $1\leqq i\leqq k$ and $C_{i,0}=0$ for $i>k$, where k is sufficiently large to produce the plateau region on the elution curve, as shown in Fig. 2.

For the self-associating system, monomer$\rightleftarrows m$-mer, we may write the equilibrium constant K in the mobile phase as

$$K=C_m/C_1^m, \tag{3}$$

where C_1 and C_m denote concentrations of the monomer and m-mer on a monomer basis. The total concentrations in the mobile and stationary phases may be written as

$$M_{i,j}=C_1+C_m=C_1+KC_1^m \tag{4}$$

and

$$S_{i,j}=P_1C_1+P_mC_m=P_1C_1+P_mKC_1^m, \tag{5}$$

where P_1 and P_m are the partition ratios for the monomer and m-mer.

Assuming appropriate values for V_0, n, P_1, P_m, K, m, and C_0, we can simulate the theoretical elution curve (C vs. V) and its first-derivative curve (dC/dV vs. V). The derivative curve provides useful information on self-associating systems.[4,10,17,18]

Asymptotic Theory. As Fig. 2 shows for the frontal method, the boundaries at the initiation (leading) and termination (trailing) of solute elution are diffuse. Approximately we may assume that the equivalent sharp boundary for the solute zone leading or trailing boundary is the first moment (centroid) of the elution profile and satisfies the relationships:

$$V_C=\int_0^{C_0} V\mathrm{d}C/C_0 \qquad \text{(leading boundary)} \tag{6}$$

and

$$V_C'=\int_0^{C_0} V\mathrm{d}C/C_0+S \qquad \text{(trailing boundary)}. \tag{7}$$

Here S is the charged volume of the sample. For these determinations the volume coordinate V is assigned a zero value when the leading boundary of the charged sample enters the column bed. This theory predicts the elution profile of a rectangle (C_0 in height and S in width) for the non-associating system.[4,16]

When this theory is applied to the self-associating system, monomer$\rightleftarrows m$-mer, we may determine the aggregation number m from the trailing boundary and the equilibrium constant K from either the leading or trailing boundary. At $m\geqq 3$, the derivative profile for the trailing boundary is expected to exhibit a min-

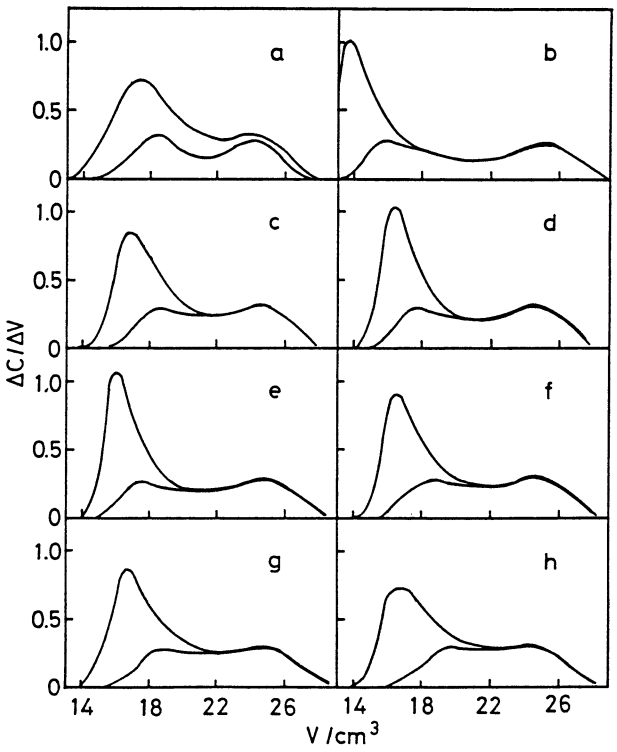

Fig. 3. Derivative chromatograms of α-chymotrypsin at concentrations of 5.0 g dm^{-3} (upper curve) and 2.4 g dm^{-3} (lower curve); Fig. a is observed[17] and Figs. b–h are calculated by using the parameters shown in Table 2.

imum (V_{min}) and two maxima ($V_{1p}>V_{mp}$), as shown in Fig. 3, and m and K may be evaluated from

$$m=(3V_{min}-V_1-2V_m)/(3V_{min}-2V_1-V_m) \quad (8)$$

and

$$K=(m-2)\{2(m^2-1)\}^{m-1}/[\{(m(2m-1)\}^m(C_{min})^{m-1}]. \quad (9)$$

Here C_{min} may be taken as the concentration corresponding to the minimum on the derivative curve and V_1 and V_m are the centroid elution volumes of the monomer and m-mer, respectively. At $m=2$, only one maximum (V_{max}') is expected for the derivative curve in the trailing boundary and K may be evaluated from

$$K=\lambda(m+\lambda)^{m-1}/(m^mC_e^{m-1}). \quad (10)$$

Here C_e may be taken as the concentration at the maximum and $\lambda=(V_1-V_{max}')/(V_{max}'-V_m)$.

For the leading boundary the centroid volume V_c may be written as

$$V_c=\alpha V_1+(1-\alpha)V_m, \quad (11)$$

where α is the weight fraction of monomeric species in the plateau region. Substitution of $C_1=C_0\alpha$ and $C_m=C_0(1-\alpha)$ into Eq. 3 yields

$$K=(1-\alpha)/(C_0^{m-1}\alpha^m), \quad (12)$$

where α may be taken as $(V_c-V_m)/(V_1-V_m)$ from Eq. 11.[3-5,16] Thus, the main advantage of the asymptotic theory over the plate theory is to provide the analytical solutions for m and K. However, the values of m and K estimated from the asymptotic theory may be used as a first approximation.

Results and Discussion

Concentration Dependence of Elution Volumes. Generally speaking, the elution volume increases with increasing solute concentration slightly.[16] In the case where the elution volume of a nonassociable solute increases with increasing concentration, the leading boundary becomes broader than the trailing one.[19] This elution pattern is the reverse found for self-associating solutes.[17]

Figure 2 shows the elution curves for ovalbumin at 1.6 g dm^{-3} and 12 g dm^{-3}. From such results V_c (and V_c') has been determined as a function of C_0:

$$V_c=18.18+0.080C_0. \quad (13)$$

In the experiments $S=12.0$ cm^3 and $V_0=12.53$ cm^3 (estimated in this work). Substitution of these values and Eq. 13 into Eq. 2 yields

$$P=0.00638C_0+0.45092. \quad (14)$$

Based on the plate theory by using P (Eq. 14), V_0 (12.53 cm^3), C_0 (1.6 or 12 g dm^{-3}) and $n=250$, we can simulate the elution curve. These theoretical curves are drawn by the dashed lines. At the low concentration of the protein, the leading and trailing boundaries are almost symmetric, whereas at the high concentration the leading boundary is broader than the trailing. These results are well reproduced, showing the utility of the plate theory to predict the shape of the elution pattern. Asymptotic theory always predicts a rectangular elution pattern for a non-associable solute. The results of Fig. 2 have also been explained by the Houghton theory.[19,20] This theory is applicable for the system where the concentration dependence of V_c is small.

Table 1. Comparison between the Observed and Theoretical Values of V_c for Dimerization of Human Carbonylhemoglobin as a Function of Concentration

C_0	V_{obsrd}[a]	V_{calc}[b]			
		Asymptotic theory		Plate theory	
mmol dm^{-3}	cm^3	K=0.25	K=0.31	K=0.25	K=0.31
0.3×10^{-6}	37.8	37.79	37.75	37.79	37.75
1	37.4	37.45	37.37	37.46	37.38
2	36.95[c]	37.15	37.05	37.16	37.05
5	36.5	36.68	36.57	36.69	36.58
8	36.45[c]	36.43	36.32	36.44	36.33
10	36.2	36.32	36.22	36.33	36.23
12	36.17[c]	36.23	36.13	36.24	36.14
14	36.2	36.15	36.06	36.17	36.07

a) Taken from Ref. 3. b) $V_1=38.0$ cm^3, $V_m=34.9$ cm^3, and $V_0=15.6$ cm^3 were used. c) Average of two or three data.

Dimerization of Carbonylhemoglobin. The equilibrium constant of dimerization of human carbonylhemoglobin has been determined from Sephadex G-200 column experiments.[3] In Table 1 the observed and theoretical V_c values from the leading boundary are shown as a function of protein concentration. From the experiments at 10^{-8} mol dm^{-3} and 10^{-3} mol dm^{-3}, the V_c values for the monomer and dimer have been estimated to be 38.0 and 34.9 cm^3, respectively. These values may be regarded as independent of concentration. The void volume has been determined to be 15.6 cm^3 from V_c of tobaco mosaic virus.[3]

By substituting m=2, the observed values of V_m, V_1, and C_0, and an assumed K value in Eq. 12, we can calculate the theoretical V_c value for dimerization. In Table 1 the calculated V_c values for two K values are shown; a K value of 0.25 dm^3 mmol^{-1} has been reported by the original workers[3] and 0.31 dm^3 mmol^{-1} is our best fitted value. A K value of 0.28 dm^3 mmol^{-1} has been estimated from porous disk diffusion measurements for the same protein.[3] Agreement between the K values estimated from the two methods is very good, showing that these values are reliable.

From the plate theory we can calculated V_c by using the observed values of V_0, V_1, and V_m and assumed values of K and n. The V_c values for the cases n=200 and K=0.25 and 0.31 are included in Table 1. Agreement between the asymptotic and plate theories is excellent.

Hexamerization of Chymotrypsin at Neutral pH. Winzor and Scheraga have reported frontal elution patterns and their derivatives for α-chymotrypsin at pH 7.9.[17] In the elution curve the leading boundary was sharper than the trailing. This feature is common for self-associating systems and is in contrast with nonassociating concentration-dependent systems, as shown in Fig. 2. This characteristic has been explained by the asymptotic theory[16] and is also explicable on the basis of the plate theory (computed results are omitted).

The derivative trailing patterns for several protein concentrations have been reported.[17] The data at two concentrations of them, 5.0 and 2.8 g dm^{-3}, are shown in Fig. 3, since most of the main features appear herein. Extrapolation of the monomer elution volume to C_0=0 permits us to estimate a value of V_1=25.0 cm^3.[3] One of the main problems encountered in the use of GFC patterns to characterize self-associating systems is the absence of the definite value of V_m.[16] As expected from Table 2, one of the estimation methods is to choose the gel phase from which the polymer is excluded.[4] Then V_m may be identified with V_0, the void volume of the column bed. By this reasoning Ackers and Thompson have taken V_m as 11.9 cm^3.[3] Substituting these values in Eq. 8, together with an estimate of V_{min}=21.5 cm^3 (inferred from Fig. 3a), they estimated a value of m=6.[3] Furthermore a C_{min} value of 1.4 g dm^{-3} has been inferred[4] from the size of the more slowly migrating part of the bimodal trailing boundary reported by Winzor and Scheraga. By using these m and C_{min} values, a K value of 0.015 dm^{15} g^{-5} has been estimated from Eq. 9.[4] However, we should be alert to the above analysis since an estimated V_0 value has been used. In this connection it is noted that the sedimentation velocity patterns of Massey et al.[21] yielded a slightly higher estimate of C_{min} (1.8 g dm^{-3}), from which a value of K=0.004 dm^{15} g^{-5} has been obtained on the basis of asymptotic theory.[4]

Table 2. Seven Sets of the Parameters to Simulate Polymerization of α-Chymotrypsin at Neutral pH on the Basis of Plate Theory[a]

Set	m	K / g^{m-1} dm^{3m-3}	V_1 / cm^3	V_m / cm^3
b	6	0.015	25.0	11.9
c	6	0.010	23.9	15.5
d	6	0.010	23.9	14.0+0.298C_m
e	6	0.009	24.5	13.2+0.357C_m
f	5	0.014	24.5	13.2+0.357C_m
g	5	0.015	24.5	14.5
h	4	0.020	24.5	12.0+0.357C_m

a) n=100 is used for simulation.

Taking these uncertainties of K and V_m values into consideration, we made simulations for many sets of the values of m, V_1, V_m, K, and n. Seven sets of them are shown in Table 2. In the following calculations, we used n=100. In set b, the values used in the above analysis based on the asymptotic theory are employed. As Fig. 3b shows, the polymer peaks have much smaller V_m values than the observed ones (Fig. 3a). This discrepancy may be ascribed to inadequate values for V_m or V_0 (or both) suggested by Ackers and Thompson. The most uncertain parameter in this simulation is V_m. Therefore we considered larger V_m values and their concentration dependences (sets c—e). Determann and Nichel reported a calibration relation between molecular weights and elution volumes for many proteins from the literature.[22] From this relation we can estimate a value of V_0=13.1 cm^3. The V_m values in Table 2 are chosen by taking this V_0 value into consideration. As Figs. 3c—e show, the simulated polymer peak at 5 g m^{-3} is slightly sharper than the observed one. Therefore we considered smaller aggregation numbers. As Fig. 3f shows, the simulated curve at C_0=2.4 g dm^{-3} gives a slightly broader peak than the observed. A value of m=5 (Figs. 3f and 3g) gives as good fittings as m=6. None of the simulations (b—h) very well reproduce the experimental result (a). This discrepancy may be ascribed to the inaccuracy in both the experimental result and the plate theory. Asymptotic theory predicts unrealistic derivative patterns.[4]

Comparison between Asymptotic and Plate Theories. In application of Eq. 8 the practical upper limit

lies in the region $m<10$, since the denominator of Eq. 8 approaches experimental errors in the determination of the elution volume.[3] Therefore we made model calculations in the case of hexamerization to compare the two theories.

For these theories we used the same parameters, viz., V_1=230.0, V_m=130.0, V_0=100.0, and K=1. Concentration dependence of these parameters was neglected. Substitution of these values and m=6 in Eqs. 8 and 9 yielded V_{min}=203.3 and C_{min}=0.649. According to the asymptotic theory, these values should be independent of C_0. Furthermore V_c for the leading boundary can be calculated from Eq. 12 and is shown in Table 3.

From the plate theory, we also calculated the frontal elution curve and its derivative, by assuming n=100. From these curves we determined several characteristic values. These are shown in Table 3. The equilibrium monomer concentration C_1 was calculated from Eq. 3 and included herein. In this table V_{mp} and V_{lp} are the elution volumes at maxima ($V_{mp}<V_{lp}$) in the trailing boundary of the derivative curve.

The V_{min} value calculated from the plate theory increases with increasing concentration, in contrast with concentration independence expected from the asymptotic theory. The experimental V_{min} data on chymotrypsin support the prediction of the plate theory (e.g., see Fig. 3). Therefore the estimation of m from Eq. 8 may be generally regarded as a first approximation. The value of C_{min} from the plate theory is also concentration-dependent and is smaller than that of the asymptotic theory. It is notable that C_{min} is smaller than C_1. Combination of Eqs. 9 and 12 yields

$$C_e/C_0=\{(m-2)(2m-2)^{m-1}\alpha^m\}^{1/(m-1)}/\{(2m^2-m)(1-\alpha)\}^{1/(m-1)}. \quad (15)$$

At the limit $m\to\infty$

$$C_{min}\to C_0\alpha=C_1. \quad (16)$$

Here the equation $C_e=C_{min}$ is used since $m\geqq 3$. The same conclusion (Eq. 16) was obtained from the plate theory based on phase separation model for micelle formation.

Table 3 shows that the plate theory predicts the increase of V_1 and the decrease of V_m with increasing concentration. Concentration dependence of the elution volume of the monomer and m-mer does not always indicate size changes of these species. These results are consistent with the experimental data on chymotrypsin.[17]

The difference between the V_c values calculated from the two theories is 0.5, regardless of C_0. Since this difference (close to $V_0/2/n$) decreases with increases in n, we can conclude that the two theories predict the same V_c value for the leading boundary. This conclusion may justify applications of the asymptotic theory to leading boundary data for self-associating systems, such as hemoglobin[1] and carbonylhemoglobin (Table 1).

Implications to Micellization of Surfactants. The above results may be useful for quantitative analyses of GFC data on surfactants. The aggregation number of surfactants is usually larger than that of proteins, e.g., typically $m>50$. Hence phase separation model ($m=\infty$) has been used to analyze GFC data for pure and mixed surfactants.[11-13] This model is useful, but is less accurate than mass action model since m is a definite value. Furthermore, most of the GFC data on surfactants have been analyzed on the basis of the asymptotic theory.[6-8]

The monomer concentration C_1 for hexaethylene glycol dodecyl ether ($C_{12}E_6$) has been estimated by two interpretations of GFC data. First approach[7] used Eq. 11 and second approach assumed the equality of $C_{min}=C_1$.[8] As expected, the former approach yielded greater C_1 values than the latter.[7,8] However, both approaches must be reconsidered, as shown below.

According to Phillips' definition of the cmc, the cmc is a C_0 value which satisfies the equation $d^3(C_1+C_m/m)/dC_0^3=0$.[23] By using this definition and Eq. 3, we can obtain

$$\text{cmc}=[Km(2m-1)/(m-2)]^{1/(1-m)}. \quad (17)$$

This equation can be also obtained from the equation $d^3C_1/dC_0^3=0$.[24] On the other hand, we can write C_{min} at $m\geqq 3$ from Eq. 9 as

$$C_{min}=\left\{\frac{K[m(2m-1)]^m}{(m-2)[2(m^2-1)]^{m-1}}\right\}^{1/(1-m)} \quad (18)$$

When m is large enough, we can thus obtain

$$C_{min}\cong\text{cmc}\cong(2Km)^{1/(1-m)}. \quad (19)$$

This equation provides the physical meaning of C_{min} and a GFC method for cmc determination without interpolation of any property. The C_{min} value for $C_{12}E_6$ increased with increasing C_0, whereas the plate theory

Table 3. Comparison between Two Theories in Hexamerization[a]

C_0	C_1	Plate theory[b]					Asymptotic theory[c]
		C_{min}	V_{min}	V_{mp}[d]	V_{lp}[d]	V_c	V_c
0.125	0.125	—[e]	—[e]	—[e]	229.8	230.5	230.0
0.25	0.250	—[e]	—[e]	—[e]	229.8	230.4	229.9
0.5	0.487	—[e]	—[e]	—[e]	230.0	227.8	227.3
1	0.778	0.624	196.5	175.2	232.1	208.3	207.8
2	1.000	0.589	203.4	146.7	233.5	180.5	180.0
4	1.188	0.587	205.0	138.0	234.3	160.2	159.7
8	1.371	0.582	206.5	134.0	235.0	147.6	147.1
16	1.560	0.581	207.5	132.5	236.0	140.3	139.8
32	1.765	0.579	208.5	131.5	236.5	136.0	135.5
64	1.990	0.576	209.3	131.2	237.0	133.6	133.1

a) V_1=230.0, V_m=130.0, V_0=100.0, and K=1 are used for calculations. b) n=100 is used. c) C_{min}=0.649 and V_{min}=203.3 were obtained from Eqs. 8 and 9, regardless of C_0. d) These values are the volumes at maxima in the derivative elution curves. e) Not observed.

predicts a slight decrease of C_{min} (e.g., see Table 3) and the asymptotic theory predicts the constancy. This discrepancy between theory and experiment may be ascribed to the increase of m with increasing C_0 for $C_{12}E_6$.[8,10]

In GFC, generally, large particles have smaller elution volumes than small ones. For self-associating systems, however, the elution volume depends on C_0 as well as size of species. As Fig. 3 shows, the polymer peak shifts toward smaller volume side with increasing C_0. This is not due to the increase of m. For $C_{12}E_6$, the elution volume of the micelle decreased with increasing C_0. This decrease has all been ascribed to the increase of m. The V_m value in Eq. 11 should correspond to true size of the micelle, and is not equal to the elution volume of the micelle at the concentration of the solution used.[10]

Conclusion

To demonstrate the scope and limitations of asymptotic theory and plate theory based on mass action law for self-associating systems, we investigated the elution patterns for ovalbumin (nonassociable protein), dimerization of carbonylhemoglobin, hexamerization of chymotrypsin, and micellization of surfactants. The asymptotic theory has an advantage of giving analytical expressions (V_c, C_{min}, V_{min}, and others) for elution patterns of self-associating systems. Equation 11, which was supported by the plate theory, gives the basis for the estimation of monomer concentrations of such systems. For surfactants C_{min} is very close to the cmc (Eq. 19). The plate theory has an advantage of requiring only a limited number of parameters over other theories.[14] It correctly predicts that the trailing boundary becomes sharper with increasing C_0 when the elution volume of a nonassociable solute increases linearly with C_0. Derivative elution profiles of self-associating systems were well simulated to make possible estimation of m and K and prediction of concentration dependence of V_{min} and C_{min}. These predictions will be useful to analyze experimental GFC data on surfactants.[18]

This work was supported by a Grant-in-Aid from the Scientific Research Foundation of Kyoto Pharmaceutical University.

References

1) R. Valdes and G. K. Ackers, *J. Biol. Chem.*, **252**, 74 (1977).
2) G. A. Gilbert, *Disc. Faraday Soc.*, **20**, 68 (1955); *Proc. R. Soc. London, Ser. A*, **250**, 377 (1959).
3) G. K. Ackers and T. E. Thompson, *Proc. Natl. Acad. Sci. U.S.A.*, **53**, 342 (1965).
4) L. W. Nichol and D. J. Winzor, "Migration of Interacting Systems," Clarendon Press, Oxford (1972), Chap. 3.
5) T. Sasaki, *Yukagaku*, **16**, 49 (1967).
6) H. Suzuki, *Bull. Chem. Soc. Jpn.*, **49**, 375 (1976).
7) T. Sasaki, M. Yasuoka, and H. Suzuki, *Bull. Chem. Soc. Jpn.*, **50**, 2538 (1977).
8) A. Goto, R. Sakura, and F. Endo, *J. Colloid Interface Sci.*, **67**, 491 (1978).
9) C. Tanford, Y. Nozaki, and M. F. Rohde, *J. Phys. Chem.*, **81**, 1555 (1977).
10) N. Funasaki, S. Hada, and S. Neya, *J. Phys. Chem.*, **92**, 3488 (1988).
11) F. Tokiwa, K. Ohki, and I. Kokubo, *Bull. Chem. Soc. Jpn.*, **41**, 2845 (1968).
12) T. Nakagawa and H. Jizomoto, *Kolloid-Z. Z. Polym.*, **234**, 1124 (1970).
13) T. Nakagawa and H. Jizomoto, "Proceedings of the IVth International Congress on Surface Active Substances," Barcelona (1968), p. 299.
14) J. L. Bethune and G. Kegeles, *J. Phys. Chem.*, **65**, 1761 (1961); J. K. Zimmerman, D. J. Cox, and G. K. Ackers, *J. Biol. Chem.*, **246**, 4242 (1971); L. M. Gilbert and G. A. Gilbert, *Methods Enzymol.*, **48**, 195 (1978); D. J. Cox, *ibid.*, **48**, 212 (1978); G. Kegeles and J. R. Cann, *ibid.*, **48**, 248 (1978).
15) A. J. P. Martin and R. L. M. Syringe, *Biochem. J.*, **35**, 1358 (1941).
16) G. K. Ackers, *Adv. Protein Chem.*, **24**, 343 (1970).
17) D. J. Winzor and H. A. Scheraga, *Biochemistry*, **2**, 1263 (1963).
18) N. Funasaki, S. Hada, and S. Neya, *J. Phys. Chem.*, in press.
19) D. J. Winzor and L. W. Nichol, *Biochim. Biophys. Acta*, **104**, 1 (1965).
20) G. Houghton, *J. Phys. Chem.*, **67**, 84 (1963).
21) V. Massey, W. F. Harrington, and B. S. Hartley, *Disc. Faraday Soc.*, **20**, 24 (1955).
22) H. Determann and W. Michel, *J. Chromatogr.*, **25**, 303 (1966).
23) J. N. Phillips, *Trans. Faraday Soc.*, **51**, 561 (1951).
24) S. Ikeda, "Colloid Chemistry," Shokabo, Tokyo (1986), Chap. 6.